PROCEEDINGS OF THE ROYAL SOCIETY B BIOLOGICAL SCIENCES

Ocean warming and acidification have complex interactive effects on the dynamics of a marine fungal disease

Gareth J. Williams, Nichole N. Price, Blake Ushijima, Greta S. Aeby, Sean Callahan, Simon K. Davy, Jamison M. Gove, Maggie D. Johnson, Ingrid S. Knapp, Amanda Shore-Maggio, Jennifer E. Smith, Patrick Videau and Thierry M. Work

Proc. R. Soc. B 2014 **281**, 20133069, published 22 January 2014

PROCEEDINGS OF THE ROYAL SOCIETY B

rspb.royalsocietypublishing.org

Research

Cite this article: Williams GJ *et al*. 2014 Ocean warming and acidification have complex interactive effects on the dynamics of a marine fungal disease. *Proc. R. Soc. B* **281**: 20133069. http://dx.doi.org/10.1098/rspb.2013.3069

Received: 23 November 2013
Accepted: 17 December 2013

Subject Areas:
ecology, health and disease and epidemiology, microbiology

Keywords:
coral reef, coralline fungal disease, ocean acidification, temperature, bio-erosion, climate change

Author for correspondence:
Gareth J. Williams
e-mail: gareth@ucsd.edu

†These authors contributed equally to this study.

Electronic supplementary material is available at http://dx.doi.org/10.1098/rspb.2013.3069 or via http://rspb.royalsocietypublishing.org.

Royal Society Publishing

Ocean warming and acidification have complex interactive effects on the dynamics of a marine fungal disease

Gareth J. Williams[1,†], Nichole N. Price[1,†], Blake Ushijima[2,4], Greta S. Aeby[4], Sean Callahan[2], Simon K. Davy[5], Jamison M. Gove[6,3], Maggie D. Johnson[1], Ingrid S. Knapp[4,5], Amanda Shore-Maggio[2,4], Jennifer E. Smith[1], Patrick Videau[2] and Thierry M. Work[7]

[1]Scripps Institution of Oceanography, Center for Marine Biodiversity and Conservation, University of California San Diego, La Jolla, CA 92093, USA
[2]Department of Microbiology, and [3]Joint Institute for Marine and Atmospheric Research, University of Hawaii at Manoa, Honolulu, HI, USA
[4]Hawaii Institute of Marine Biology, Kaneohe, HI 96744, USA
[5]School of Biological Sciences, Victoria University of Wellington, PO Box 600, Wellington, New Zealand
[6]Coral Reef Ecosystem Division (CRED), Pacific Islands Fisheries Science Center (PIFSC), NOAA, 1610 Kapiolani Boulevard, Suite 1110, Honolulu, HI 96814, USA
[7]US Geological Survey, National Wildlife Health Center, Honolulu Field Station, PO Box 50167, Honolulu, HI 96850, USA

Diseases threaten the structure and function of marine ecosystems and are contributing to the global decline of coral reefs. We currently lack an understanding of how climate change stressors, such as ocean acidification (OA) and warming, may simultaneously affect coral reef disease dynamics, particularly diseases threatening key reef-building organisms, for example crustose coralline algae (CCA). Here, we use coralline fungal disease (CFD), a previously described CCA disease from the Pacific, to examine these simultaneous effects using both field observations and experimental manipulations. We identify the associated fungus as belonging to the subphylum *Ustilaginomycetes* and show linear lesion expansion rates on individual hosts can reach 6.5 mm per day. Further, we demonstrate for the first time, to our knowledge, that ocean-warming events could increase the frequency of CFD outbreaks on coral reefs, but that OA-induced lowering of pH may ameliorate outbreaks by slowing lesion expansion rates on individual hosts. Lowered pH may still reduce overall host survivorship, however, by reducing calcification and facilitating fungal bio-erosion. Such complex, interactive effects between simultaneous extrinsic environmental stressors on disease dynamics are important to consider if we are to accurately predict the response of coral reef communities to future climate change.

1. Introduction

Diseases alter ecosystems [1] and threaten marine community function and resilience [2]. On coral reefs, disease outbreaks are considered a key contributor to the recent global decline of reef health and resilience [3]. Both global impacts, for example sea-surface temperature anomalies, and local human impacts, for example pollution, drive disease dynamics and outbreaks in scleractinian corals on reefs [4,5]. These stressors probably increase pathogen virulence and reduce host resistance, enhancing disease establishment and progression [2,6]. Our understanding of diseases that threaten other key calcifying (reef-building) organisms, however, is rudimentary. Crustose coralline algae (CCA) serve essential functional roles in coral reef ecosystems, including facilitating reef accretion and consolidation [7], providing a settlement substrate for coral larvae [8] and forming a key successional state promoting reef recovery following acute disturbance [9]. While CCA can occupy up to 50% of the living reef

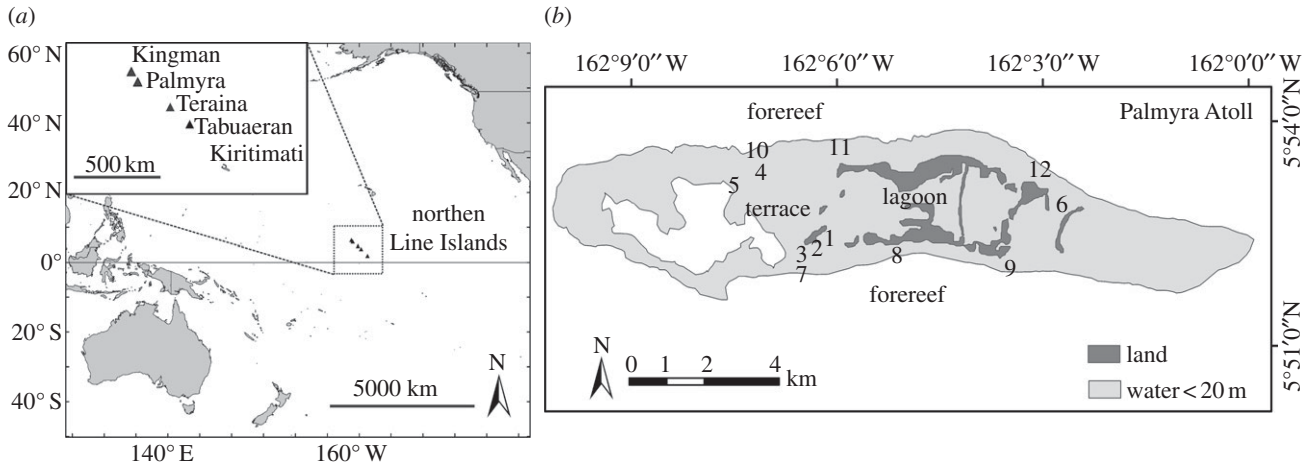

Figure 1. Location of Palmyra Atoll and the permanent monitoring sites established in 2008 (1–5 = shallow terrace; 6 = backreef; 7–12 = forereef).

benthos [7,10], relatively little is known about their biology and ecology [11], particularly their susceptibility to and subsequent impacts from disease [12].

Diseases can cause drastic reductions in CCA populations on coral reefs, with knock-on effects that promote regime shifts to fleshy macroalgal dominance and loss of functional resilience [13–15]. Several CCA diseases have been documented, although almost nothing is known about their aetiology, spatio-temporal dynamics and relationships with extrinsic environmental drivers [12]. This information is essential if we are to actively manage CCA disease occurrence and mitigate outbreaks at a local scale on coral reefs. While CCA are able to photoacclimatize [16], they are still vulnerable to bleaching as a result of increased temperature, and their calcification, photophysiology and survival are threatened by a lowering of pH and carbonate saturation state (Ω) as a result of ocean acidification (OA) [17–19]. However, the influence of these global-scale stressors on local-scale CCA disease dynamics and occurrence on coral reefs is virtually unknown. Here, using a CCA disease previously described from the South Pacific, we shed light on this urgent research priority for, to our knowledge, the first time.

Coralline fungal disease (CFD) was first observed in 1997 on shallow (less than 20 m) reef habitats in American Samoa. Based on gross morphology, the aetiology of the disease was identified as an undescribed fungal pathogen [20]. Since 1997, CFD has been documented throughout other parts of the Pacific, with high prevalence at remote islands in the Central Pacific, in particular at Kingman Reef and Palmyra Atoll in the northern Line Islands [12]. While the distribution of CFD throughout the Pacific appears to be highly variable, evidence suggests that variations in sea-surface temperature (SST) may, in part, be driving spatial variation in disease occurrence, with higher mean SST at islands correlating with higher CFD occurrence [12]. However, the principal environmental drivers of temporal variation in CFD occurrence remain unknown.

In late 2009, a well-developed El Niño resulted in anomalous ocean warming across the equatorial Pacific Ocean. The sustained increase in temperature resulted in coral-bleaching events and disease outbreaks at some of the Pacific's most remote coral reef systems, including Palmyra Atoll, where CFD is prevalent [21–23]. Using time-series field observations at Palmyra before, during and after the 2009–2010 El Niño ocean-warming event, followed by experimental manipulations, we show that CFD temporal dynamics are driven by variations in seawater temperature and that spatial variation in disease occurrence appears independent of host abundance. We show that CFD can exhibit very rapid progression across hosts, rivalling known rates for coral diseases and that increased temperature accelerates CFD lesion progression. We show that these effects are counteracted by a reduction in pH; however, under simulated OA conditions, diseased hosts still experience greater rates of net dissolution than healthy individuals. These complex interactions highlight the challenges associated with predicting disease outbreaks and their dynamics in a changing climate.

2. Material and methods

(a) Histopathology

Fragments ($n = 7$, approx. 3 cm^2) of CCA displaying gross signs of CFD were collected at Palmyra Atoll (05°52′ N, 162°06′ W), at 10 m depth on the forereef (figure 1). Each sample was fixed in zinc–formaldehyde solution (Z-fix, Anatech) diluted 1 : 5 with ambient non-filtered seawater, decalcified using a formic acid/formaldehyde solution (Cal-Ex II, Fisher Scientific), embedded in paraffin, sectioned at 5 µm and stained with haematoxylin and eosin. Grocott's methenamine silver was used to confirm the presence of fungal hyphae.

(b) Culture conditions and phylogenetic determination of coralline fungal disease fungus

(i) Culture conditions

To culture the fungus associated with CFD, Medium B, Wickerham's, Czapek-Dox agar and cellulose agar [24] prepared with 25, 50, 75 or 100% filtered seawater as a base were used. Media were prepared with and without the inclusion of the antibiotics ampicillin and spectinomycin at a concentration of 100 µg ml^{-1}. Media with antibiotics were used to suppress bacterial growth, and the same media were used without antibiotics to preclude any potential negative effects on fungal growth. Solid media included 0.7, 1.0, 1.2 or 1.5% agar (Fisher Scientific). Cultures were incubated at 25, 27 or 30°C with aeration (solid cultures) or without aeration (liquid cultures) for 21 days.

(ii) DNA extraction and gene amplification

Frozen, ground CFD lesions were thawed on ice, 5 µl were spread on PALM PEN membrane slides (Carl Zeiss) and individual fungal filaments were isolated with a Zeiss PALM laser microdissection system. DNA was extracted from filaments as in [25] with the following modifications: two samples of 8–10 fungal filaments in 50 µl of sterile water were lysed with a mini-beadbeater (Biospec) and extracted with phenol–chloroform. DNA was

precipitated, dried and re-suspended in 20 µl of sterile 10 mM Tris buffer, pH 8.5. A 719 bp fragment of the 18S rRNA gene was PCR amplified with fungus-specific primers designed from mixed environmental samples: nu-SSU-0817–5′ and nu-SSU-1536–3′ [26] and Phusion high-fidelity polymerase (New England Biolabs). The same primers were used for sequencing.

(iii) Phylogenetic analysis

The fungal 18S rRNA gene sequence was initially assessed using The National Center for Biotechnology Information (NCBI) and the BLAST algorithm. To further assess its relatedness to other phylum *Basidiomycota* members, especially the subphylum *Ustilaginomycetes*, 653 bp 18S rRNA gene sequences were aligned in MEGA5 [27]. The fungal isolate's sequence was aligned with 22 other NCBI sequences, chosen based on a previously published analysis of the phylum *Basidiomycota* [28], using ClustalW. A phylogenetic tree was constructed using the neighbour-joining method with 1000 bootstrap replicates [29]. All positions containing gaps and missing data were eliminated, leaving a total of 647 positions. Evolutionary distances (number of base substitutions per site) were computed using the maximum composite likelihood method. Rate variation among sites was modelled with a gamma distribution (shape parameter = 8). Evolutionary analyses were conducted in MEGA5.

(c) Coralline fungal disease occurrence, host cover and associated changes in seawater temperature

To quantify CFD occurrence, 59 × 200 m^2 transects were surveyed in July–August and October–November 2008 (total of 11 800 m^2 of reef). Backreef ($n = 4$ transects, 1–5 m depth), reef terrace ($n = 25$, 4–5 m depth) and forereef ($n = 30$, 10 m depth) habitats were surveyed within 12 permanent sites (figure 1). Along each transect, per cent CCA cover was estimated using the photoquadrat method. Each photoquadrat ($n = 20$ per 50 m) was 0.63 m^2. Per cent cover was calculated post hoc by identifying 100 points in a stratified random design for each photograph and averaging within each transect. Difficulties with delineating individual CCA crusts *in situ* meant a true CFD prevalence (proportion of individuals displaying signs of the disease) could not be calculated. Instead, the numbers of CFD cases were normalized to host cover (per m^2 of CCA) along each transect (see the electronic supplementary material, table S1 for mean raw number of CFD cases and per cent cover of CCA within each transect over time). Forty of the 59 transects surveyed in 2008 became permanent as part of the Palmyra disease monitoring programme and were resurveyed for CFD occurrence and CCA cover in October–November 2009 and March 2010.

Throughout the study, *in situ* forereef temperature data were sampled at 30 min intervals at 10 m depth using Sea-Bird Electronics (SBE 39) temperature sensors with a resolution and accuracy of 0.0001°C and ±0.002°C, respectively. Satellite-derived weekly SST and long-term monthly climatological SST for Palmyra were calculated following [30].

(d) Coralline fungal disease vital rates during the El Niño

On the central south forereef, 13 CFD cases were photographed weekly for four weeks in October–November 2009. Individual CFD cases were initially marked with a stainless steel pin as a reference point. Photographs were taken perpendicular to the substrate to minimize angle variations among images. CFD vital rates (lesion surface area and linear progression rate) were calculated post hoc using ImageJ (http://rsbweb.nih.gov/ij). Active lesion surface area was the area displaying fungal cover (blue–black discoloration), not including dead CCA left in the lesion's path. Calculations were averaged across three images of each lesion to account for slight variations in angle among photos.

(e) Temperature and acidification experiments

We used a factorial CO_2 bubbling and heating experiment (3–13 June 2012) to examine independent and interactive effects of OA and warming on CFD disease dynamics (lesion surface area and linear progression rate) and CCA growth (net calcification). Samples were collected, as for histopathology, from independent diseased and healthy CCA crusts. Epiphytes were removed, and each CCA genus was confirmed using a dissecting microscope. Paired CCA fragments (approx. 2 cm^2 *Neogoniolithon* sp.; diseased and healthy) were placed in 1 l glass aquaria holding fresh seawater equilibrated to treatment conditions (approx. 24–48 h before) (*sensu* [31]). Experimental OA conditions were created by bubbling pre-mixed air enriched with excess pCO_2 (AirGas Pro) to 1124 ± 88 µatm (mean ± s.e. hereafter) to reflect atmospheric CO_2 concentrations projected in 2100 (scenario IV; [32]). In control aquaria, present-day CO_2 conditions were created using a Pacbrake 12 V HP625 air compressor delivering ambient air. Aquaria were immersed in flow-through water baths at 28.06 ± 0.01°C (seasonal average for Palmyra; ambient conditions) or 29.49 ± 0.02°C (mean SST during the El Niño warming event at Palmyra; warming conditions). Four independent water baths (two ambient and two warmed) held experimental aquaria that were randomly assigned to elevated or present-day CO_2 conditions to create every combination of warming and OA treatment level ($n = 12$ per level divided evenly among the two water baths).

Aquaria were covered to prevent evaporation and rainwater from affecting salinity and placed under a shade cloth to mimic the natural light environment at 10 m on the forereef. To control for algal metabolism, two empty aquaria per water bath were subjected to the same four treatments described above. In each aquarium, temperature and light conditions were recorded every 15 min using Onset HOBO Pendant UA-002-64 light and temperature loggers (see the electronic supplementary material, figure S1). Light intensities (lux) were converted to the availability of photosynthetically active radiation (PAR) using the equation: 1 µmol quanta (400–700 nm) $m\,s^{-1} = 51.2$ lux (*sensu* [33]). These conversions were validated by midday PAR measurements with an Li-Cor LI 192 4π quantum sensor (492 ± 25 µmol photons $m\,s^{-1}$). Once daily, $pH_{seawater}$ (resolution ± 0.01), temperature (±0.1°C) and dissolved oxygen (±0.2 mg l^{-1}; electronic supplementary material, table S2) were monitored using an HACH HQ 40d handheld meter. These measurements were also taken at 6.00, 12.00, 18.00 and 24.00 h to quantify diurnal fluctuations in each aquarium (see the electronic supplementary material, table S2). Twelve water samples for total alkalinity (A_T), total dissolved inorganic carbon (C_T) and salinity were collected at days 2, 6 and 10 of the experiment in 500 ml Corning brand Pyrex bottles and fixed with 200 µl saturated $HgCl_2$ solution (1% headspace). Samples were collected (in duplicate) from experimental aquaria and control (empty) aquaria at each of the four treatment levels.

(f) Crustose coralline algae calcification and disease progression

Net calcification rates of all fragments of *Neogoniolithon* sp. were quantified with the buoyant weight method [34] (to the nearest mg) using a weigh-below basket on a balance (Denver SI-403). Changes in buoyant weight over the 10 day experiment, normalized to initial fragment mass, approximated net calcification rate. For each diseased fragment, CFD disease vital rates (lesion surface area and linear progression rate) were calculated using ImageJ as described above.

(g) Experimental water chemistry analysis

Carbonate chemistry and salinity were analysed in the Dickson Laboratory at Scripps Institution of Oceanography. C_T was determined using a single-operator multiparameter metabolic

analyser (SOMMA) and a UIC Model 5011 CO_2 coulometer. A_T was determined by open-cell acid titration using a Metrohm Dosimat Model 665 and Metrohm potentiometric pH probe and meter. Salinity was determined using a Mettler Toledo Model DE45 density meter. Seawater dissolved inorganic carbon parameters (HCO_3^-, CO_3^{2-}, CO_2, pCO_2) and the saturation state of carbonate minerals (Ω-calcite and Ω-Mg calcite) were calculated based on measured C_T and A_T using the computer program SEACARB [35] and stoichiometric dissociation constants [36] (see the electronic supplementary material, table S3).

(h) Data analyses

To test for differences in CCA cover and CFD occurrence across forereef sites in 2008, we ran a permutation-based analysis of variance and subsequent pairwise comparisons using PERMANOVA+ [37]. To test for any relation between CCA abundance and CFD occurrence in 2008, we used a permutational linear model using Distlm_*forward* [38]. Two-way nested analyses of variance (ANOVAs) tested whether OA (fixed) and warming (fixed) treatments independently or jointly affected net calcification; each fixed factor had two levels. Replicates from a water bath were nested within temperature treatments to test for location bias. Analyses were run independently for diseased and healthy samples. Normality and homoscedasticity were verified using the Shapiro–Wilk test. Growth responses were compared between diseased and healthy CCA within each treatment using *t*-tests. Proportional changes in lesion area were analysed using the Dunn's method for joint ranking, a non-parametric approach that compares means of treatments against a control (ambient SST and air); we confirmed that variances across treatments were equal with a Brown–Forsythe test. Unless otherwise stated, all analyses were completed using R 2.15.2 (R Development Core Team, http://www.r-project.org).

3. Results

(a) Coralline fungal disease gross morphology and histopathology; phylogeny of associated fungus

CFD lesions were characterized by a diffuse area of mottled white discoloration separated from a pink CCA thallus by a blue–black band (approx. 1–3 cm wide) with irregular distinct undulating borders (figure 2*a*). Septated hyphae with branches originating near septal junctions were commonly observed (figure 2*b*). Many of the fungal filaments had highly branched structures resembling conidiophores, which in some cases appeared to have attached spherical conidia, the asexual spores of fungi. These were the dominant fungal structures in diseased CCA but were absent in healthy CCA. The CCA cuticle was overlaid and disrupted by mats of brown to colourless filamentous branching septate structures (figure 2*c*). These irregularly walled structures infiltrated into the CCA thallus at right angles to the cuticle to a depth of approximately 100 µm. These were morphologically compatible with fungi, and Grocott's methenamine silver confirmed a fungal infection (figure 2*c*).

Isolation by microdissection followed by genetic sequencing of the fungal hyphae revealed that 653 bp of the 18S rRNA gene sequence (accession no. KF255580) shared 97–98% sequence identity with members of the phylum *Basidiomycota* and uncultured marine isolates. The sequence was most similar (98% sequence identity) to members of the subphylum *Ustilaginomycetes*, in particular *Malassezia restricta* strain CBS-7877 and the marine isolates KM10-BASS and CK2-BASS (see the electronic supplementary material, figure S2). Repeated attempts to culture the fungus were unsuccessful.

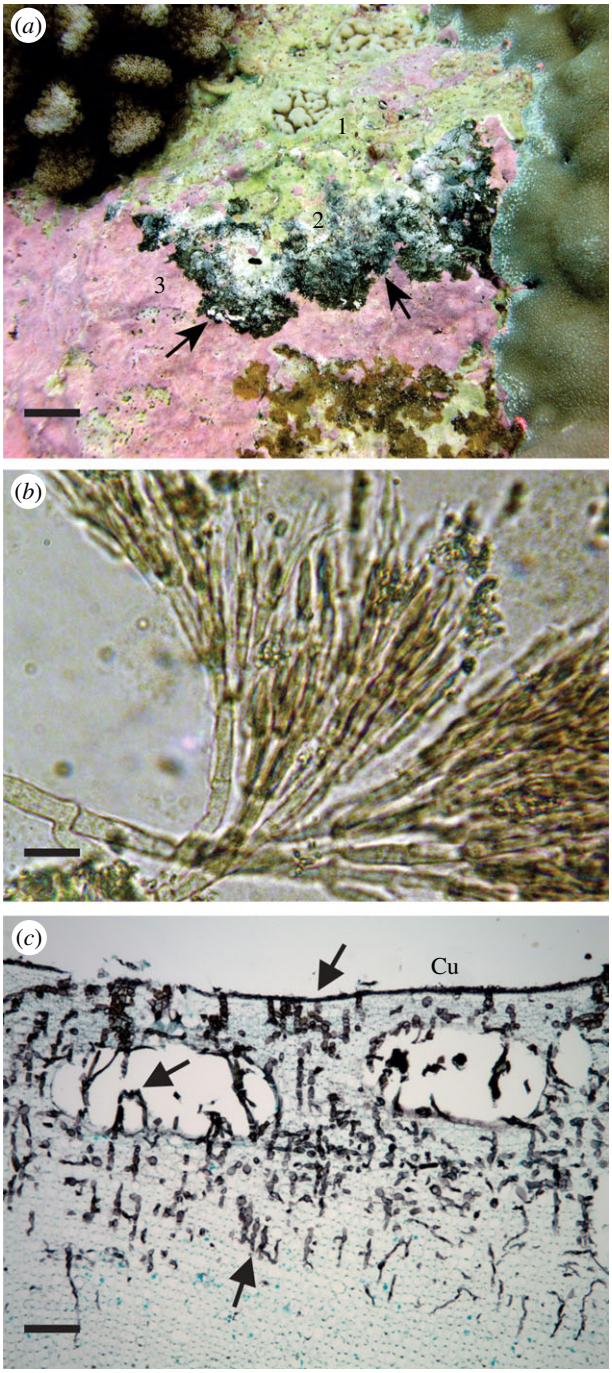

Figure 2. (*a*) Field signs of CFD. The active lesion is shown by the two black arrows. Day-old exposed substrate becomes colonized by microalgae and turf algae (1) and appears bleached white when freshly exposed (2), while the CCA tissue remains healthy looking on the leading edge of the lesion (3). Scale bar, 1 cm. (*b*) Appearance of isolated fungal hyphae associated with CFD (1000× magnification using light microscopy). Scale bar, 15 µm. (*c*) Section of a coralline algal infected with CFD and positively confirmed as a fungal infection using Grocott's methenamine silver. Note the fungal hyphae invading the algal thallus and conceptacles (arrows). Cu, cuticle. Scale bar, 30 µm. (Online version in colour.)

(b) Spatio-temporal patterns of coralline fungal disease and associated changes in seawater temperature

Atoll-wide mean (±1 s.e.) CFD occurrence on Palmyra's forereef habitat equalled 0.1 ± 0.06 cases m^{-2} of CCA in 2008

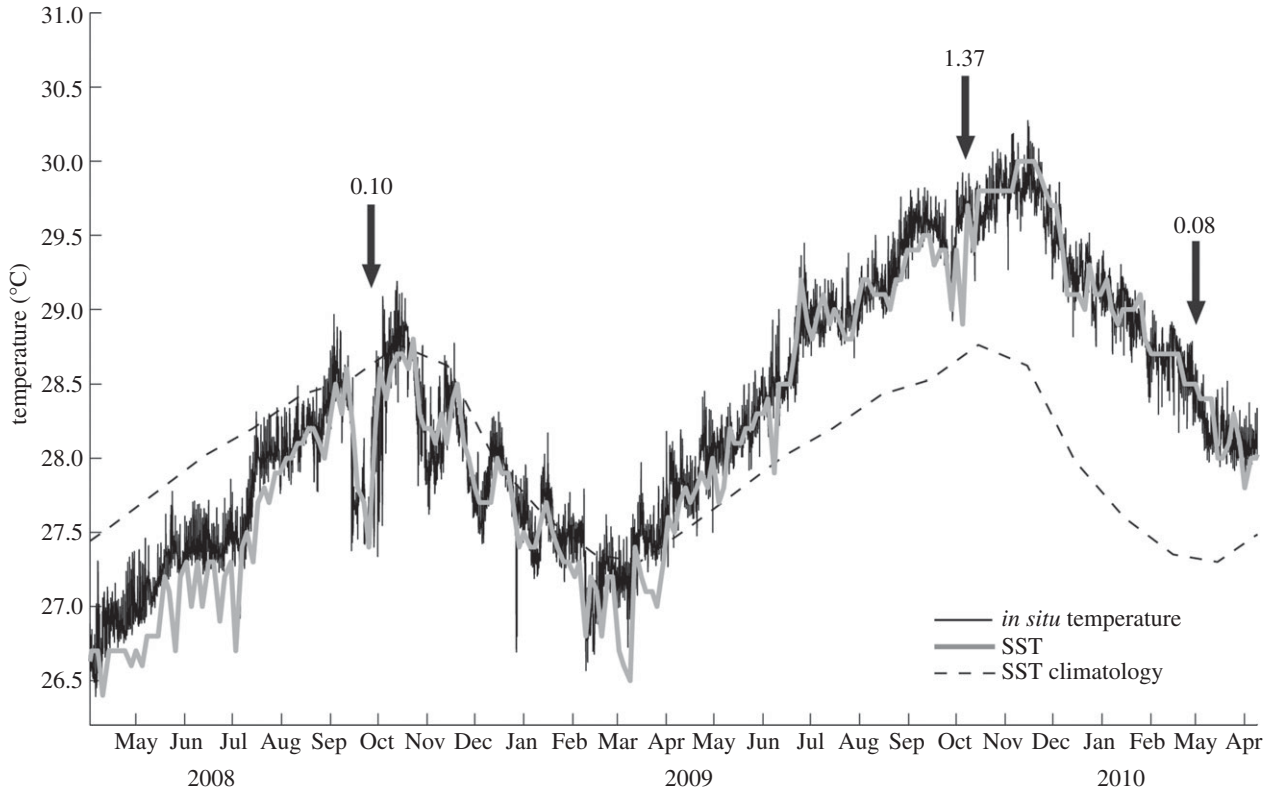

Figure 3. Representative *in situ* temperatures at Palmyra Atoll at 10 m on the forereef and SST from satellite-derived sources during 2008, 2009 and 2010, and the associated change in CFD occurrence (forereef-wide mean number of cases m^{-2} of CCA are shown by black arrows).

(total reef area surveyed in this habitat equalled 6000 m^2). Although cases of CFD were seen outside of our surveyed transects on the deeper (approx. 10–15 m) reef terrace habitat, cases were rare in comparison; no CFD cases were documented within our surveyed transects on the shallow (less than 5 m) terrace or backreef habitats (total reef area surveyed in these two habitats equalled 5800 m^2). Within the forereef habitat, CFD occurrence displayed spatial heterogeneity (Pseudo-$F_{5,29} = 13.456$, $p < 0.0001$), with the central south forereef having the highest mean number of cases m^{-2} of CCA (0.39 ± 0.10) in 2008 (see the electronic supplementary material, table S1). Per cent cover of CCA did not differ across forereef sites in 2008 (Pseudo-$F_{5,29} = 2.67$, $p = 0.06$, mean cover 23.5%), and there was no relationship between CFD occurrence and CCA cover (Pseudo-$F_{1,29} = 0.311$, $p = 0.751$; electronic supplementary material, table S1).

Within the permanent backreef and reef terrace transects, mean CFD occurrence remained at 0 cases m^{-2} of CCA in 2009 and 2010. However, within the permanent forereef transects, CFD mean occurrence increased approximately 14-fold from 0.10 cases m^{-2} of CCA in 2008 to 1.37 cases m^{-2} of CCA in late 2009 in association with the El Niño ocean-warming event (figure 3; electronic supplementary material, table S1). Seawater temperature had steadily increased over the latter part of 2009 and eventually peaked in November 2009, reaching 1.25 and 1.51°C (satellite and forereef temperature observations, respectively) above the maximum long-term monthly climatological SST for Palmyra (figure 3). CFD occurrence increased in all permanent forereef transects during the El Niño event, with the central south forereef maintaining the highest levels (3.74 cases m^{-2} of CCA; electronic supplementary material, table S1). By March 2010, with a decrease in seawater temperatures, mean forereef CFD occurrence had returned to pre-El Niño levels (figure 3).

(c) Coralline fungal disease vital rates during the El Niño event

CFD lesions typically progressed in a radial manner across the surface of the CCA thallus, often crossing between individual CCA thalli but never spreading onto hard coral tissue (see the electronic supplementary material, figure S3). At time point zero, mean lesion surface area of the 13 CFD cases *in situ* was 108 mm^2 (± 25) (see the electronic supplementary material, table S4). After one week, mean lesion surface area was 136 mm^2 (± 23), with a mean surface area progression rate of 3.5 $mm^2\ d^{-1}$ (± 2.3) and a mean linear progression rate of 2.4 mm d^{-1} (± 0.5). Across the entire four-week time period, the maximum surface area progression rate and linear progression rate of any single CFD lesion was 12.9 $mm^2\ d^{-1}$ and 6.5 mm d^{-1}, respectively (see the electronic supplementary material, table S4).

(d) Experimental effects of warming and acidification on crustose coralline algae calcification and disease progression rates

Exposure to elevated temperature and atmospheric pCO_2, designed to simulate OA, reduced CCA net calcification rates, but this effect was dependent on fungal infection (table 1). All CCA samples gained $CaCO_3$ mass in the ambient air treatments, while all samples lost mass in the elevated pCO_2 (lower pH) treatments (figure 4*a*). However, when exposed to both elevated pCO_2 and temperature, diseased CCA lost nearly

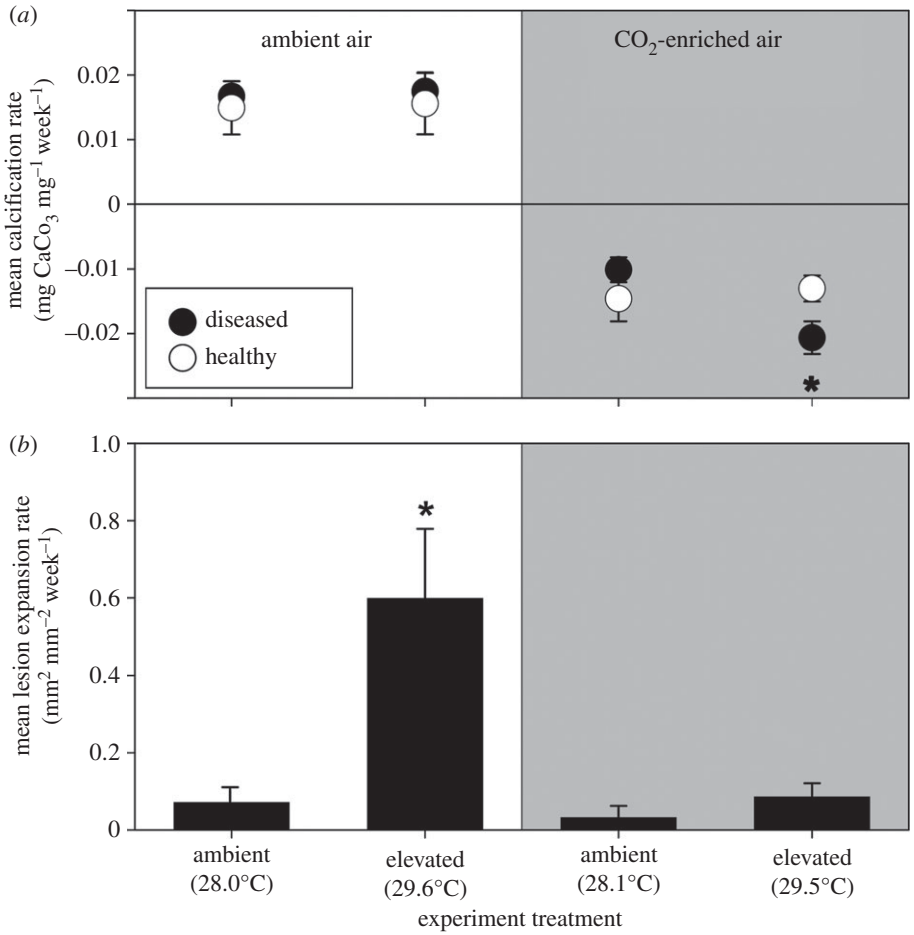

Figure 4. (*a*) Mean (±s.e.) calcification rate for diseased and healthy CCA in experimental aquaria ($n = 12$). Change in weight shown as mg $CaCO_3$ $week^{-1}$ for each thallus. Asterisk indicates when response within treatment differs significantly between diseased and healthy specimens (table 1). (*b*) Mean (±s.e.) lesion lateral expansion rate for diseased CCA in experiments. Using the ambient air × 28°C treatment as a control value, the asterisk indicates a significant effect of elevated temperature (Dunn's $Z = 3.156$, $p = 0.0048$).

Table 1. Two-way ANOVA results for calcification rates of diseased and healthy CCA crusts ($n = 8$ per treatment) immersed in the OA ('CO_2 enrichment') and ambient conditions across duplicate flow-through seawater tables ('table') nested within a warming El Niño ('temperature') or a seasonal average scenario.

CCA state	source	d.f.	*F*	*p*
healthy, no lesions	CO_2 enrichment	1	64.327	<0.0001
	temperature	1	0.018	0.896
	CO_2 × temperature	1	0.050	0.824
	table (temperature)	2	1.667	0.208
diseased, lesions present	CO_2 enrichment	1	163.153	<0.0001
	temperature	1	3.008	0.095
	CO_2 × temperature	1	4.593	0.042
	table (temperature)	2	0.396	0.677

twice as much mass as when exposed to simulated OA alone (significant interaction term, table 1). Mass loss was not intensified for healthy CCA (figure 4*a*); net calcification rates in healthy CCA were significantly depressed only by elevated pCO_2 and not by elevated temperature (table 1). Accordingly, calcification rates for diseased and healthy samples were statistically similar in all treatments, except for the simultaneous acidified and warmed conditions, in which diseased CCA lost 40% more mass than healthy CCA (*t*-test, d.f. = 15, $p = 0.0343$). Visible lateral progression of the CFD lesion occurred only in the elevated temperature treatment in ambient CO_2 conditions where lesion size and lethality increased by 60% over one week (figure 4*b*).

4. Discussion

Using a previously described CCA fungal disease (CFD) [20], we demonstrate that ocean warming and acidification can have complex interactive effects on marine disease dynamics. These

relationships are to be expected, as they reflect intricate relationships among the putative pathogen, host and environment [39].

(a) Identification of coralline fungal disease-associated fungus

Fungal pathogens are prevalent throughout the marine environment [40,41], are commonly associated with the coral holobiont [42] and are known to infect tropical sea-fans [43,44] and marine algae [45]. An inability to culture fungal isolates and a reliance on morphology for identification, however, have caused fungal isolates to be misclassified and their distribution underestimated [46]. Using histopathology of CFD samples from Palmyra Atoll and genetic sequencing of the associated fungus, we confirm a fungal infection of the CCA. While species-level identification was not possible, our phylogenetic analysis strongly suggests that the CFD fungus belongs to the subphylum *Ustilaginomycetes*, which consists of a large number of plant parasites, including strains of smut fungi [47]. Our methods, which allowed isolation of the fungus without an axenic culture, could be used to compare the fungus present in the Palmyra CFD lesions with fungi associated with suspected CFD lesions found on other reefs. These genetic approaches allow us to better interpret spatio-temporal dynamics of this disease on coral reefs and postulate their underlying mechanisms.

(b) Disease dynamics and sea-surface temperature

Many fungal pathogens in animals and plants respond positively to elevated temperatures [48–51], and ocean warming is predicted to favour pathogens for many marine diseases [2]. At our study location, CFD displayed a dramatic (14-fold) increase in occurrence on the forereef during an El Niño in association with sustained seawater temperatures well above the long-term climatological mean. Furthermore, we found experimentally that elevated temperature increases lateral expansion rates of CFD lesions. The positive relationship between temperature and CFD occurrence was probably the result of elevated temperatures increasing the virulence of the pathogen, and hence speeding disease progression and causing physiological stress to the CCA host that ultimately reduced resistance to infection [52]. The prevalence of many coral diseases, such as white syndromes [5], atramentous necrosis [53] and black band disease [54] are also positively related to temperature. Interestingly, Vargas-Ángel [12] documented higher overall CCA disease occurrence at islands experiencing higher mean annual SST in a Pacific-wide survey of US-affiliated coral reefs, further highlighting the importance of temperature in governing CCA disease dynamics.

Though temperature variation provides a strong explanation for temporal variation in overall CFD occurrence at our study location, it does not adequately explain the spatial variation we documented at any one point in time. If higher temperatures cause both CFD occurrence and rates of lesion progression to increase, why was the disease almost exclusively limited to the forereef, where temperatures are lower than the shallow reef terrace [21]? There are several possible explanations. Host density is often a crucial factor determining the spatio-temporal distribution patterns of disease [39], with the prevalence of many coral and CCA diseases positively related to host abundance [5,55,56]. For example, Vargas-Ángel [12] found a positive relationship between island mean CCA cover and overall CCA disease occurrence at an archipelago scale across coral reefs of the US Pacific, including the Pacific Remote Island Areas, the geopolitical region within which Palmyra resides. However, within Palmyra's forereef habitat, CFD occurrence appeared to be independent of host abundance. Moreover, CCA cover peaks on Palmyra's shallow (less than 5 m) western reef terrace [10], where CFD was virtually absent; previous surveys at Palmyra have documented CFD on the terrace habitat, but again at deeper (approx. 15 m) depths (B. Vargas-Ángel 2013, personal communication) where host cover is lower [10]. These findings suggest that host abundance alone does not explain the observed spatial variation in CFD occurrence at Palmyra. However, CCA species assemblages are known to vary spatially on reefs [57], and the peak of CFD occurrence on the forereef may simply reflect an increase in the abundance of a preferred host species. While *in situ* species-specific assessments of CCA abundance would potentially resolve these issues, CCA taxonomy is difficult and requires microscopic examination, making it impossible in the field.

While potentially explaining between-habitat differences in disease occurrence, variation in host species abundance alone does not adequately explain the dramatic peak in CFD abundance on Palmyra's central south forereef. This CFD hotspot at Palmyra appears to be temporally stable, corroborating previous surveys conducted in 2006 [12]. The existence of this CFD hotspot at one site suggests that disease occurrence may be governed by external inputs of the pathogen, rather than by within-population transmission [44], or by an unmeasured extrinsic forcing. Palmyra's central south forereef is exposed to a particularly high level of lagoonal outflow during the change in tidal state (G. J. Williams 2007–2013, personal observation), perhaps acting as a pathogen source and/or supplying more nutrient-rich waters that may enhance CFD establishment and progression, as has been shown for other fungal diseases on coral reefs [4]. Additionally, the south forereef of Palmyra has, on average, measurably higher seawater pH with less frequent or severe excursions than the north forereef or reef terrace [58]; our results indicate that the less acidic but warmer conditions characteristic of the southern forereef are most favourable for CFD occurrence. Regardless of the mechanisms behind the fine-scale variations in CFD occurrence, it is clear that the disease is more abundant and virulent under elevated temperatures, suggesting that predicted increases in the frequency of temperature anomalies on coral reefs may result in more frequent CFD outbreaks.

(c) Eco-physiological response of host to disease and climate change

What will be the ecological consequences of increased CFD outbreaks on coral reefs? While elevated temperature increased overall CFD occurrence *in situ* and lateral rates of lesion expansion under experimental conditions, under the same experimental conditions elevated pCO_2 mediated these effects of temperature and slowed lesion expansion rates. While this suggests that future increases in the frequency of temperature anomalies will result in more frequent CFD outbreaks on coral reefs, the lowering of pH as a result of OA may actually slow down overall spread of the disease across the reef landscape during such outbreaks. Importantly, however, while the lateral spread of CFD was not affected by reduced seawater pH and carbonate saturation state, all CCA thalli lost mass under OA conditions, suggesting that net dissolution was occurring. For diseased thalli, these effects were exacerbated by warming.

Synergistic effects of ocean warming and acidification that together cause greater reduction in calcification of CCA than either stressor alone have been reported elsewhere [17–19,59], but synergistic global climate change effects were only observed in this study when the CCA were also infected with the CFD fungus. Microboring organisms, or euendoliths, such as fungi or cyanobacteria, burrow and erode carbonate at rates that can exceed biogenic $CaCO_3$ precipitation, leading to the net dissolution of reef-building organisms [60,61]. OA is expected to reduce resistance to eudondolith penetration in both hermatypic corals and CCA by weakening structural integrity of the $CaCO_3$ crystals [62], reducing skeletal density [63] and facilitating chemical dissolution [64,65]. Further, the colony formation is stimulated by natural reductions in pH, so OA has the potential to radically elevate the abundance of marine fungi [66]. Not only can acidification weaken host resistance to bio-erosion, but also reduced saturation states and enhanced disease infestation of the CCA thallus could further accelerate corrosion. Thus, the synergistic interaction of pathogen infection, warming and OA may exacerbate reef degradation under projected global climate change scenarios.

(d) Conclusion

Our study represents, to our knowledge, the first attempt to understand the interactive effects of two major global stressors, ocean warming and acidification, on disease dynamics on coral reefs. Using a fungal disease affecting crustose coralline algae (CFD), we show that while outbreaks of CFD should become more common on coral reefs as temperature anomalies become more frequent, OA may ameliorate lesion progression rates but still decrease overall survivorship of diseased hosts. The ecological consequences of such interactions are difficult to predict; however, it is clear that CFD possesses a tremendous capacity for lateral spread across the reef landscape during ocean-warming events. Our results highlight the intricate nature of disease–host–environment interactions and the importance of adopting a multi-factor approach to modelling disease dynamics on coral reefs in order to accurately predict dynamics in a changing climate.

Acknowledgements. We thank the US Fish and Wildlife Service (USFWS) and The Nature Conservancy for granting access to Palmyra Atoll and providing logistical support. We thank Rachel Morrison for edits to the manuscript and Brian Zgliczynski for logistical support. We additionally thank two anonymous reviewers for comments that greatly improved this manuscript. The majority of this research was conducted under the USFWS special use permits 12533-10010, 12533-11025, and 12533-12012. Scripps Institution of Oceanography is a member of the Palmyra Atoll Research Consortium (PARC). This is PARC publication number PARC-0098.

Funding statement. Funding was provided by the National Geographic Society, the Gordon and Betty Moore Foundation and a Victoria University of Wellington (VUW) Strategic Research Scholarship.

References

1. Ward JR, Lafferty KD. 2004 The elusive baseline of marine disease: are diseases in ocean ecosystems increasing? *PLoS Biol.* **2**, 542–547. (doi:10.1371/journal.pbio.0020120)
2. Harvell CD, Mitchell CE, Ward JR, Altizer S, Dobson AP, Ostfeld RS, Samuel MD. 2002 Ecology: climate warming and disease risks for terrestrial and marine biota. *Science* **296**, 2158–2162. (doi:10.1126/science.1063699)
3. Aronson RB, Precht WF. 2001 White-band disease and the changing face of Caribbean coral reefs. *Hydrobiologia* **460**, 25–38. (doi:10.1023/A:10131 03928980)
4. Bruno JF, Petes LE, Harvell CD, Hettinger A. 2003 Nutrient enrichment can increase the severity of coral diseases. *Ecol. Lett.* **6**, 1056–1061. (doi:10.1046/j.1461-0248.2003.00544.x)
5. Bruno JF, Selig ER, Casey KS, Page CA, Willis BL, Harvell CD, Sweatman H, Melendy AM. 2007 Thermal stress and coral cover as drivers of coral disease outbreaks. *PLoS Biol.* **5**, 1220–1227. (doi:10.1371/journal.pbio.0050124)
6. Harvell D, Jordan-Dahlgren E, Merkel S, Rosenberg E, Raymundo L, Smith G, Weil E, Willis B, Global Envrionment Facility C. 2007 Coral disease, environmental drivers, and the balance between coral microbial associates. *Oceanography* **20**, 172–195. (doi:10.5670/oceanog.2007.91)
7. Littler MM, Littler DS. 1984 Models of tropical reef biogenesis. *Phycol. Res.* **3**, 324–364.
8. Price N. 2010 Habitat selection, facilitation, and biotic settlement cues affect distribution and performance of coral recruits in French Polynesia. *Oecologia* **163**, 747–758. (doi:10.1007/s00442-010-1578-4)
9. Nyström M, Graham NAJ, Lokrantz J, Norström AV. 2008 Capturing the cornerstones of coral reef resilience: linking theory to practice. *Coral Reefs* **27**, 795–809. (doi:10.1007/s00338-008-0426-z)
10. Williams GJ, Smith JE, Conklin EJ, Gove JM, Sala E, Sandin SA. 2013 Benthic communities at two remote Pacific coral reefs: effects of reef habitat, depth, and wave energy gradients on spatial patterns. *PeerJ.* **1**, e81. (doi:10.7717/peerj.81)
11. Chisholm JR. 2003 Primary productivity of reef-building crustose coralline algae. *Limnol. Oceanogr.* **48**, 1376–1387. (doi:10.4319/lo.2003.48.4.1376)
12. Vargas-Angel B. 2010 Crustose coralline algal diseases in the U.S.-affiliated Pacific Islands. *Coral Reefs* **29**, 943–956. (doi:10.1007/s00338-010-0646-x)
13. Littler MM, Littler DS. 1995 Impact of CLOD pathogen on Pacific coral reefs. *Science* **267**, 1356–1360. (doi:10.1126/science.267.5202.1356)
14. Littler MM, Littler DS. 1997 Disease-induced mass mortality of crustose coralline algae on coral reefs provide a rationale for conservation of herbivorous fish stocks. In *Proc. 8th Int. Coral Reef Symp.*, vol. 1 (eds HA Lessions, IG Macintyre), pp. 719–724.
15. Goreau TJ *et al*. 1998 Rapid spread of diseases in Caribbean coral reefs. *Rev. Biol. Trop.* **46**, 157–171.
16. Bulleri F. 2006 Duration of overgrowth affects survival of encrusting coralline algae. *Mar. Ecol. Prog. Series* **321**, 79–85. (doi:10.3354/meps321079)
17. Anthony KRN, Kline DI, Diaz-Pulido G, Dove S, Hoegh-Guldberg O. 2008 Ocean acidification causes bleaching and productivity loss in coral reef builders. *Proc. Natl Acad. Sci. USA* **105**, 17 442–17 446. (doi:10.1073/pnas.0804478105)
18. Martin S, Gattuso JP. 2009 Response of Mediterranean coralline algae to ocean acidification and elevated temperature. *Glob. Change Biol.* **15**, 2089–2100. (doi:10.1111/j.1365-2486.2009.01874.x)
19. Johnson MD, Carpenter RC. 2012 Ocean acidification and warming decrease calcification in the crustose coralline alga *Hydrolithon onkodes* and increase susceptibility to grazing. *J. Exp. Mar. Biol. Ecol.* **434**, 94–101. (doi:10.1016/j.jembe.2012.08.005)
20. Littler MM, Littler DS. 1998 An undescribed fungal pathogen of reef-forming crustose coralline algae discovered in American Samoa. *Coral Reefs* **17**, 144. (doi:10.1007/s003380050108)
21. Williams GJ, Knapp IS, Maragos JE, Davy SK. 2010 Modeling patterns of coral bleaching at a remote Central Pacific atoll. *Mar. Pollut. Bull.* **60**, 1467–1476. (doi:10.1016/j.marpolbul.2010.05.009)
22. Williams GJ, Knapp IS, Work TM, Conklin EJ. 2011 Outbreak of *Acropora* white syndrome following a mild bleaching event at Palmyra Atoll, northern Line Islands, Central Pacific. *Coral Reefs* **30**, 621. (doi:10.1007/s00338-011-0762-2)

23. Vargas-Angel B, Looney EE, Vetter OJ, Coccagna EF. 2011 Severe, widespread El Nino-associated coral bleaching in the US Phoenix Islands. *Bull. Mar. Sci.* **87**, 623–638. (doi:10.5343/bms.2010.1095)
24. Kjer J, Debbab A, Aly AH, Proksch P. 2010 Methods for isolation of marine-derived endophytic fungi and their bioactive secondary products. *Nat. Protoc.* **5**, 479–490. (doi:10.1038/nprot.2009.233)
25. Campbell EL, Summers ML, Christman H, Martin ME, Meeks JC. 2007 Global gene expression patterns of *Nostoc punctiforme* in steady-state dinitrogen-grown heterocyst-containing cultures and at single time points during the differentiation of akinetes and hormogonia. *J. Bacteriol.* **189**, 5247–5256. (doi:10.1128/JB.00360-07)
26. Borneman J, Hartin RJ. 2000 PCR primers that amplify fungal rRNA genes from environmental samples. *Appl. Environ. Microbiol.* **66**, 4356. (doi:10.1128/AEM.66.10.4356-4360.2000)
27. Tamura K, Peterson D, Peterson N, Stecher G, Nei M, Kumar S. 2011 MEGA5: Molecular evolutionary genetics analysis using maximum likelihood, evolutionary distance, and maximum parsimony methods. *Mol. Biol. Evol.* **28**, 2731–2739. (doi:10.1093/molbev/msr121)
28. Bass D *et al*. 2007 Yeast forms dominate fungal diversity in the deep oceans. *Proc. R. Soc. B* **274**, 3069–3077. (doi:10.1098/rspb.2007.1067)
29. Tamura K, Nei M, Kumar S. 2004 Prospects for inferring very large phylogenies by using the neighbor-joining method. *Proc. Natl Acad. Sci. USA* **101**, 11 030–11 035. (doi:10.1073/pnas.0404206101)
30. Gove JM, Williams GJ, McManus M, Heron S, Sandin SA, Vetter OJ, Foley D. 2013 Quantifying climatological ranges and anomalies for Pacific coral reef ecosystems. *PLoS ONE* **8**, e61974. (doi:10.1371/journal.pone.0061974)
31. Price NN, Hamilton SL, Tootell JS, Smith JE. 2011 Species-specific consequences of ocean acidification for the calcareous tropical green algae *Halimeda*. *Mar. Ecol. Prog. Ser.* **440**, 67–78. (doi:10.3354/meps09309)
32. IPCC. 2007 IPCC Fourth Assessment Report: climate change 2007 (eds Core writing team, RK Pachauri, A Reisinger). Geneva, Switzerland: IPCC.
33. Valiela I. 1984 *Marine ecological processes*. New York, NY: Springer.
34. Davies PS. 1989 Short term growth measurements of corals using an accurate buoyant weighing technique. *Mar. Biol.* **101**, 389–395. (doi:10.1007/BF00428135)
35. Lavigne H, Gattuso JP. 2011 seacarb: seawater carbonate chemistry with R. (R package v. 2.4 edn). (http://CRANR-project.org/package=seacarb)
36. Lueker TJ, Dickson AG, Keeling CD. 2000 Ocean pCO_2 calculated from dissolved inorganic carbon, alkalinity, and equations for K-1 and K-2: validation based on laboratory measurements of CO_2 in gas and seawater at equilibrium. *Mar. Chem.* **70**, 105–119. (doi:10.1016/s0304-4203(00)00022-0)
37. Anderson MJ, Gorley RN, Clarke KR. 2008 *PERMANOVA+ for PRIMER: guide to software and statistical methods*. Plymouth, UK: PRIMER-E.
38. Anderson MJ. 2003 *DISTLM forward: a FORTRAN computer program to calculate a distance-based multivariate analysis for a linear model using forward selection*. Auckland, New Zealand: University of Auckland.
39. Ostfeld RS, Keesing F, Eviner VT. 2008 *Infectious disease ecology: the effects of ecosystems on disease and of disease on ecosystems*, p. 506. Princeton, NJ: Princeton University Press.
40. Rheinheimer G. 1992 *Aquatic microbiology*. New York, NY: Wiley.
41. Ramaiah N. 2006 A review on fungal diseases of algae, marine fishes, shrimps and corals. *Indian J. Mar. Sci.* **35**, 380–387.
42. Williams GJ, Work TM, Aeby GS, Knapp IS, Davy SK. 2011 Gross and microscopic morphology of lesions in Cnidaria from Palmyra Atoll, Central Pacific. *J. Invert. Pathol.* **106**, 165–173. (doi:10.1016/j.jip.2010.08.002)
43. Smith GW, Ives LD, Nagelkerken IA, Ritchie KB. 1996 Caribbean sea-fan mortalities. *Nature* **383**, 487–487. (doi:10.1038/383487a0)
44. Kim K, Harvell CD. 2004 The rise and fall of a six-year coral-fungal epizootic. *Am. Nat.* **164**, S52–S63. (doi:10.1086/424609)
45. Raghukumar C. 1996 Zoosporic fungal parasites of marine biota. In *Advances in zoosporic fungi* (ed. R Dayal), pp. 61–83. New Delhi, India: M D Publications Pvt. Ltd.
46. Hawksworth DL, Rossman AY. 1997 Where are all the undescribed fungi? *Phytopathology* **87**, 888–891. (doi:10.1094/phyto.1997.87.9.888)
47. Bauer R, Begerow D, Oberwinkler E, Piepenbring M, Berbee ML. 2001 Ustilaginomycetes. In *Systematics and evolution* (eds D McLaughlin, E McLaughlin, P Lemke), pp. 57–83. Berlin, Germany: Springer.
48. Bemis DA, Krahwinkel DJ, Bowman LA, Mondon P, Kwon-Chung KJ. 2000 Temperature-sensitive strain of *Cryptococcus neoformans*: producing hyphal elements in a feline nasal granuloma. *J. Clin. Microbiol.* **38**, 926–928.
49. Spitzer ED, Keath EJ, Travis SJ, Painter AA, Kobayashi GS, Medoff G. 1990 Temperature-sensitive variants of *Histoplasma capsulatum* isolated from patients with acquired immunodeficiency syndrome. *J. Infect. Dis.* **162**, 258–261. (doi:10.1093/infdis/162.1.258)
50. Hill RA, Blankenship PD, Cole RJ, Sanders TH. 1983 Effects of soil moisture and temperature on prehavest invasion of peanuts by the *Aspergillus flavus* group and subsequent aflatoxin development. *Appl. Environ. Microbiol.* **45**, 628–633.
51. Marin S, Sanchis V, Magan N. 1995 Water activity, temperature, and pH effects on growth of *Fusarium moniliforme* and *Fusarium proliferatum* isolates from maize. *Can. J. Microbiol.* **41**, 1063–1070. (doi:10.1139/m95-149)
52. Blanford S, Thomas MB, Pugh C, Pell JK. 2003 Temperature checks the Red Queen? Resistance and virulence in a fluctuating environment. *Ecol. Lett.* **6**, 2–5. (doi:10.1046/j.1461-0248.2003.00387.x)
53. Jones RJ, Bowyer J, Hoegh-Guldberg O, Blackall LL. 2004 Dynamics of a temperature-related coral disease outbreak. *Mar. Ecol. Prog. Ser.* **281**, 63–77. (doi:10.3354/meps281063)
54. Sato Y, Bourne DG, Willis BL. 2009 Dynamics of seasonal outbreaks of black band disease in an assemblage of *Montipora* species at Pelorus Island (Great Barrier Reef, Australia). *Proc. R. Soc. B* **276**, 2795–2803. (doi:10.1098/rspb.2009.0481)
55. Aeby GS *et al*. 2011 Growth anomalies on the coral genera *Acropora* and *Porites* are strongly associated with host density and human population size across the Indo-Pacific. *PLoS ONE* **6**, e16887. (doi:10.1371/journal.pone.0016887)
56. Myers RL, Raymundo LJ. 2009 Coral disease in Micronesian reefs: a link between disease prevalence and host abundance. *Dis. Aquat. Organ.* **87**, 97–104. (doi:10.3354/dao02139)
57. Dethier MN, Paull KM, Woodbury MM. 1991 Distribution and thickness patterns in subtidal encrusting algae from Washington. *Bot. Mar.* **34**, 201–210. (doi:10.1515/botm.1991.34.3.201)
58. Price NN, Martz TR, Brainard RE, Smith JE. 2012 Diel variability in seawater pH relates to calcification and benthic community structure on coral reefs. *PLoS ONE* **7**, e43843. (doi:10.1371/journal.pone.0043843)
59. Diaz-Pulido G, Anthony KRN, Kline DI, Dove S, Hoegh-Guldberg O. 2012 Interactions between ocean acidification and warming on the mortality and dissolution of coralline algae. *J. Phycol.* **48**, 32–39. (doi:10.1111/j.1529-8817.2011.01084.x)
60. Godinot C, Tribollet A, Grover R, Ferrier-Pages C. 2012 Bioerosion by euendoliths decreases in phosphate-enriched skeletons of living corals. *Biogeosciences* **9**, 2377–2384. (doi:10.5194/bg-9-2377-2012)
61. Tribollet A, Payri C. 2001 Bioerosion of the coralline alga *Hydrolithon onkodes* by microborers in the coral reefs of Moorea, French Polynesia. *Oceanol. Acta* **24**, 329–342. (doi:10.1016/s0399-1784(01)01150-1)
62. Ragazzola F, Foster LC, Form A, Anderson PSL, Hansteen TH, Fietzke J. 2012 Ocean acidification weakens the structural integrity of coralline algae. *Glob. Change Biol.* **18**, 2804–2812. (doi:10.1111/j.1365-2486.2012.02756.x)
63. Hernandez-Ballesteros LM, Elizalde-Rendon EM, Carballo JL, Carricart-Ganivet JP. 2013 Sponge bioerosion on reef-building corals: dependent on the environment or on skeletal density? *J. Exp. Mar. Biol. Ecol.* **441**, 23–27. (doi:10.1016/j.jembe.2013.01.016)
64. Tribollet A, Atkinson MJ, Langdon C. 2006 Effects of elevated pCO_2 on epilithic and endolithic metabolism of reef carbonates. *Glob. Change Biol.* **12**, 2200–2208. (doi:10.1111/j.1365-2486.2006.01249.x)
65. Wisshak M, Schonberg CHL, Form A, Freiwald A. 2012 Ocean acidification accelerates reef bioerosion. *PLoS ONE* **7**, e45124. (doi:10.1371/journal.pone.0045124)
66. Krause E, Wichels A, Giménez L, Gerdts G. 2013 Marine fungi may benefit from ocean acidification. *Aquat. Microb. Ecol.* **69**, 59–67. (doi:10.3354/ame01622)